PERGAMON

International Journal of Solids and Structures 40 (2003) 343–360

INTERNATIONAL JOURNAL OF SOLIDS and STRUCTURES

www.elsevier.com/locate/ijsolstr

About the dynamic strength enhancement of concrete-like materials in a split Hopkinson pressure bar test

Q.M. Li [a,*], H. Meng [b]

[a] *Department of Mechanical, Aerospace and Manufacturing Engineering, UMIST, P.O. Box 88, Manchester M60 1QD, UK*
[b] *School of Civil and Environmental Engineering, Nanyang Technological University, Nanyang Avenue, Singapore 639798, Singapore*

Received 8 January 2002; received in revised form 19 September 2002

Abstract

Split Hopkinson pressure bar (SHPB) technique has been used widely to measure the dynamic strength enhancement of concrete-like materials at high strain-rate between 10^1 and 10^3 s^{-1}. Although SHPB technique has been verified for metallic materials, the validity and accuracy of SHPB results for non-metallic materials have not been thoroughly studied. The present paper examines the application of SHPB to determine the dynamic strength of concrete-like materials whose compressive strength is hydrostatic-stress-dependent. It shows that the apparent dynamic strength enhancement beyond the strain-rate of 10^2 s^{-1} is strongly influenced by the hydrostatic stress effect due to the lateral inertia confinement in a SHPB test. This apparent dynamic strength enhancement has been wrongly interpreted as strain-rate effect and has been adopted in both dynamic structural design and concrete-like material models for analytical and numerical simulations, which may lead to over-prediction on the dynamic strength of concrete-like materials. The SHPB test is simulated in the present paper using FE method and Drucker–Prager model to investigate how the hydrostatic stress affects the SHPB test results of concrete-like materials. A rate-insensitive material model is used in order to examine this pseudo-strain-rate sensitive phenomenon. A collection of SHPB test results of concrete-like materials are compared with simulation results, which confirms quantitatively that the apparent dynamic strength enhancement of concrete-like materials in a SHPB test is caused by the lateral inertia confinement instead of the strain-rate sensitivity of the tested material.

Keywords: Split Hopkinson pressure bar; FE simulation; Strain-rate effects; Drucker–Prager model; Concrete-like material; Lateral inertia confinement effect

1. Introduction

The strain-rate effect on the strength of various concrete-like materials, e.g., concrete, mortar and geo-materials, has become an important factor in both the material model and the design of structures that may experience high strain-rate in a range of applications when impact or blast loading is involved. It is

* Corresponding author. Tel.: +44-161-200-5740; fax: +44-161-200-3849.
E-mail address: qingming.li@umist.ac.uk (Q.M. Li).

0020-7683/02/$ - see front matter © 2002 Elsevier Science Ltd. All rights reserved.
PII: S0020-7683(02)00526-7

generally accepted that there is an apparent increase of the dynamic strength when the concrete-like material is subjected to high strain-rate. The dynamic increase factor (DIF), defined by the ratio of the dynamic strength to the quasi-static strength in uniaxial compression, has been widely accepted as an important parameter to measure the strain-rate effect on the strength of concrete-like materials.

The dynamic strength enhancement of concrete has attracted great interest in structural design and analysis due to the broad applications of concrete in impact and blast loading environment. European CEB recommended DIF formulas for concrete in both tension and compression (Comite Euro-International du Beton, 1993), which take bilinear relations between DIF and $\log(\dot{\varepsilon})$ with a change in slope at strain-rate of 30 s^{-1}. A great number of tests have been conducted to find the dependence of DIF on strain-rate by using various test methods, e.g., drop-hammer techniques, servo-hydraulic loading rigs, split Hopkinson pressure bar (SHPB) and explosive devices. A critical review on the compressive behaviour of concrete at high strain-rates was conducted by Bischoff and Perry (1991), where various experimental techniques and test results were summarized. Williams (1994) gave a comprehensive review about the strain-rate effects on the compressive strength of concrete, where DIF measured by various researchers was plotted against the strain-rate from quasi-static to 10^2 s^{-1} for concrete of quasi-static strength between 16.5 and 103 MPa.

Although it has been shown that DIF increases 50% in average when strain-rate varies from 10^{-5} to 10^1 s^{-1}, as shown in Fig. 1, it has great uncertainty about the test results and their interpretations (Bischoff and Perry, 1991). These uncertainties may come from following sources, (1) different testing techniques; (2) specimen size effect; (3) material differences, e.g., concrete quality, aggregate grade, curing and moisture condition, age, etc., and (4) dynamic and boundary effects. It is interesting to know whether the test results

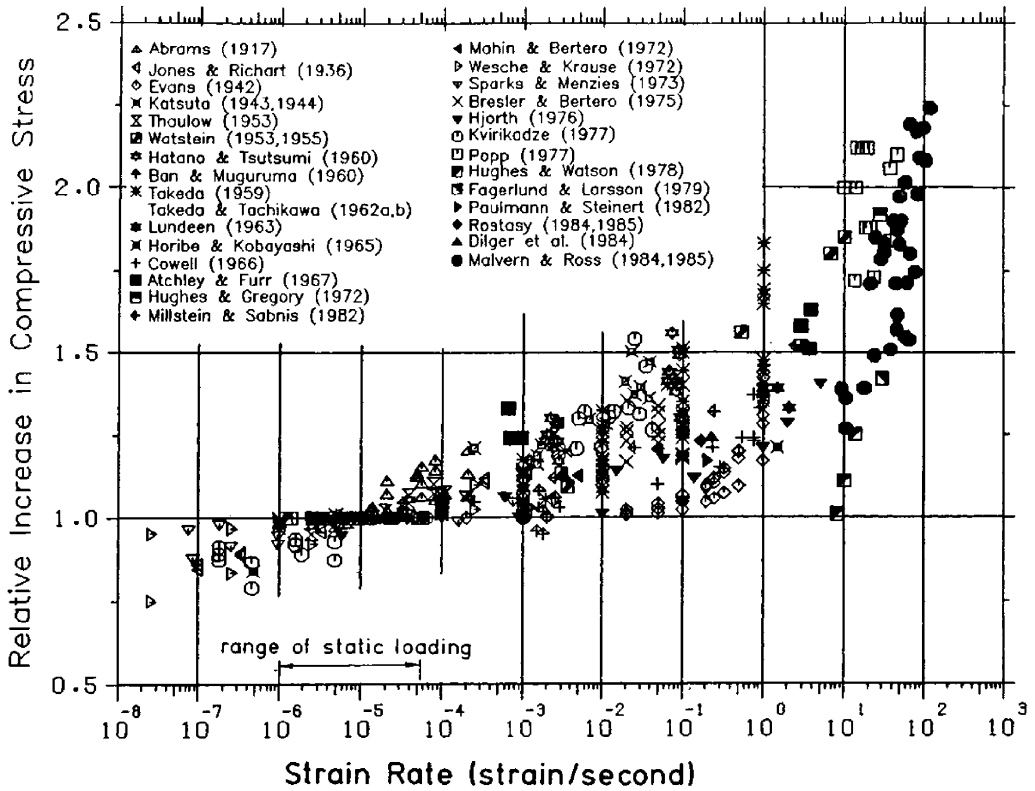

Fig. 1. Strain-rate influence on the compressive strength of concrete (Bischoff and Perry, 1991).

at high strain-rates purely reflect the strain-rate-dependence of material itself, or the dynamic effects due to the test set-up and the method of measurement have great influence on the strain-rate-sensitivity of concrete-like materials.

Comparative studies on the dynamic strength of concrete should be based on consistent experimental results, preferably from a systematic and consistent test program, in order to reduce experimental uncertainties to minimum. In recent years, SHPB technique, which was developed originally to test the dynamic stress–strain relation of metallic specimens, has been widely applied to study the dynamic compressive strength of concrete at high strain-rate from 10^1 to 10^3 s^{-1}. The SHPB-based experimental results suggested that the strain-rate influence on DIF becomes significant when the strain-rate is beyond a critical value between 10^1 and 10^2 s^{-1} (Malvern and Ross, 1985; Tedesco and Ross, 1998; Grote et al., 2001), which will be studied in the present paper.

The objective of the present study is to verify the validity of SHPB technique for testing concrete-like materials. It shows that the strain-rate-dependence of DIF obtained from SHPB tests is mainly caused by the existence of lateral inertia confinement in a SHPB test, and thus, the DIF obtained using the conventional SHPB technique should be modified to eliminate the lateral inertia confinement effect.

2. SHPB technique and strain-rate effect on DIF of concrete

2.1. SHPB technique and its limitations

A SHPB system consists of incident and transmitter pressure bars with a short specimen sandwiched between them. Three waves are involved in a SHPB test, i.e., an incident compressive pulse generated by the impact of a striker, a reflected tensile pulse due to the low impedance of the specimen and a transmitted compressive wave. Stress wave reflects at interfaces between specimen and pressure bars to homogenize the stress distribution in the specimen (Davies and Hunter, 1963). According to one-dimensional stress-wave theory, the engineering stress, strain-rate and strain defined on specimen length are

$$\sigma = \frac{P_1 + P_2}{2A_0}, \quad \dot{\varepsilon} = \frac{V_1 - V_2}{L_0} \quad \text{and} \quad \varepsilon = \int_0^t \dot{\varepsilon}\,\mathrm{d}t, \tag{1a–c}$$

where P_1 and P_2 are the forces acting on the two interfaces between the specimen and the incident/transmitter pressure bars. V_1 and V_2 are the particle velocities at the interfaces between the incident/transmitter pressure bars and the specimen, and L_0 and A_0 are the original length and area of the specimen, respectively. These values can be obtained from strain gauge stations on the incident and transmitter pressure bars.

There are two fundamental postulates for the valid application of Eq. (1) to obtain engineering stress, strain and strain-rate in the specimen, i.e.,

(1) one-dimensional elastic stress wave theory is valid in pressure bars;
(2) stress and strain states within the specimen are uniaxial and uniform.

The first postulate can be satisfied by limiting the impact velocity to ensure that the pressure bars deform elastically and by using a proper length–to–diameter ratio of pressure bars and projectile to eliminate other negative effects, e.g., wave dispersion, which will not be discussed in the present paper. The stress and strain states in a specimen are affected by several factors, e.g., the radial, or the lateral, inertia effect, the axial inertia effect and the friction restraint between the specimen and the pressure bars, which may cause the violation of the second postulate of a SHPB test. A number of researches have been published to verify the

validity of SHPB measurement for metallic specimens. For example, Bell (1966) showed that there are large discrepancies between the axial strain measured on the radial surface of the specimen and the average strain obtained from SHPB formula, Eq. (1c), when lubrication is not applied on the interfaces between specimen and pressure bars. Davies and Hunter (1963) showed that the slenderness ratio plays opposite roles on axial and lateral inertia effects and an optimal slenderness ratio exists

$$\lambda = \frac{L_0}{d} = \frac{1}{2}\sqrt{3\nu_s} \tag{2}$$

to minimize their compound influence on the accuracy of a SHPB test, where ν_s is an effective Poisson's ratio of the specimen under the experimental condition. ν_s ranges from 0.33 to 0.5 for metals deformed from elastic to plastic ranges, and thus, the optimal slenderness ratio is between 0.5 and 0.61 according to Eq. (2) to minimize the inertia effects on the accuracy of a SHPB test. Eq. (2) has been recognized as the optimal slenderness ratio for all kinds of metal specimens in a SHPB test. Meanwhile, it is also used to determine the slenderness ratio of non-metallic specimens in SHPB tests.

A numerical simulation was conducted by Bertholf and Karnes (1975) to study the accuracy of a SHPB test. A strain-rate-insensitive stress–strain relation of the specimen material was examined and the reconstituted stress–strain relation using SHPB formulae was compared with the input stress–strain curve. It was shown that serious stress and strain non-uniformity exists when the interfaces between the specimen and the pressure bars are not lubricated properly, which results in a noticeable over-prediction about the strain-rate effect due to the friction restraint at interfaces.

However, conclusions for metallic specimens may not be applicable for concrete-like specimens, mainly due to their brittleness and hydrostatic-stress-dependent behaviour, which will be discussed in Section 2.3.

2.2. DIF of concrete using SHPB technique

The dynamic strength increase in concrete was first observed by Abrams (1917) and it has been generally accepted that concrete and concrete-like materials, e.g., mortar and geomaterials, are strain-rate sensitive and the constitutive model of such materials under dynamic loading should include strain-rate effect. A large number of experiments have been performed under controlled conditions in order to quantify strain-rate effects. Research works were concentrated mostly on the compressive strength (Fu et al., 1991a,b; Bischoff and Perry, 1991), which covered a wide range of concrete of different quasi-static strengths (f_{cs}) and strain-rates, showing an obviously strength enhancement at strain-rates above a critical value.

In recent years, SHPB technique, which was developed originally to test dynamic stress–strain relation of metallic specimens, has been widely applied to study the dynamic compressive strength of concrete at high strain-rate from 10^1 to 10^3 s^{-1} (Goldsmith et al., 1966; Malvern and Ross, 1985; Ross et al., 1989; Tang et al., 1992; Zhao, 1998; Ross et al., 1995; Tedesco and Ross, 1998; Grote et al., 2001). SHPB-based experimental results suggested that the strain-rate influence on DIF becomes significant when the strain-rate is greater than a critical value that is in the range of 10^1–10^2 s^{-1} (Malvern and Ross, 1985; Tedesco and Ross, 1998; Grote et al., 2001). The details about SHPB and its limitations are given in Section 2.1. Several publications of SHPB experimental results on concrete and mortar are discussed in this section.

For strain-rates in the range of 10^1–10^3 s^{-1}, SHPB seems to be the most adequate means to test the strain-rate effect for concrete and concrete-like materials. The dependence of DIF on strain-rate was recommended by CEB for concrete, i.e.,

$$\mathrm{DIF} = \frac{f_{cd}}{f_{cs}} = \left[\frac{\dot{\varepsilon}}{\dot{\varepsilon}_s}\right]^{1.026\alpha_s} \quad \text{for} \quad \dot{\varepsilon} \leqslant 30\ s^{-1} \tag{3a}$$

and

$$\mathrm{DIF} = \gamma_s \left[\frac{\dot{\varepsilon}}{\dot{\varepsilon}_s}\right]^{\frac{1}{3}} \quad \text{for} \quad \dot{\varepsilon} > 30\ \mathrm{s}^{-1} \tag{3b}$$

where f_{cs} and f_{cd} are the unconfined uniaxial compressive strength in quasi-static and dynamic loading, respectively. $\gamma_s = 10^{(6.156\alpha_s - 2.0)}$, $\alpha_s = 1/(5 + 9f_{cs}/f_{co})$, $\dot{\varepsilon}_s = 30 \times 10^{-6}\ \mathrm{s}^{-1}$ and $f_{co} = 10$ MPa. Eq. (3b) at strain-rate above 30 s^{-1} fits Malvern and Ross (1985)'s SHPB test results (Bischoff and Perry, 1991).

A series of SHPB tests have been conducted by Ross et al. (1989, 1995, 1996) and Tedesco and Ross (1998) using SHPB for different concrete strengths, moistures and strain-rates around $10^2\ \mathrm{s}^{-1}$. A DIF regression equation was suggested as follows Tedesco and Ross (1998)

$$\mathrm{DIF} = 0.00965 \log \dot{\varepsilon} + 1.058 \geqslant 1.0 \quad \text{for} \quad \dot{\varepsilon} \leqslant 63.1\ \mathrm{s}^{-1} \tag{4a}$$

and

$$\mathrm{DIF} = 0.758 \log \dot{\varepsilon} - 0.289 \leqslant 2.5 \quad \text{for} \quad \dot{\varepsilon} > 63.1\ \mathrm{s}^{-1} \tag{4b}$$

in which the transition point from a low strain-rate sensitivity to high strain-rate sensitivity occurs at 63.1 s^{-1}, which is slightly higher than the transition point given by CEB formulae in Eqs. (3a) and (3b).

Recently, Grote et al. (2001) tested mortar on SHPB from 250 to 1700 s^{-1} strain-rate. A sharp increase of DIF was observed at strain-rate around $10^2\ \mathrm{s}^{-1}$. Following formulae is suggested to measure the dependence of DIF on strain-rate

$$\mathrm{DIF} = 0.0235 \log \dot{\varepsilon} + 1.07 \quad \text{for} \quad \dot{\varepsilon} \leqslant 266.0\ \mathrm{s}^{-1} \tag{5a}$$

and

$$\mathrm{DIF} = 0.882(\log \dot{\varepsilon})^3 - 4.4(\log \dot{\varepsilon})^2 + 7.22(\log \dot{\varepsilon}) - 2.64 \quad \text{for} \quad \dot{\varepsilon} > 266.0\ \mathrm{s}^{-1}. \tag{5b}$$

Above SHPB test results are demonstrated in Fig. 2, which clearly indicates there is a sharp increase of DIF beyond a transition point of strain-rate around $10^2\ \mathrm{s}^{-1}$ for concrete or concrete-like materials. It is interested to find the possible causes responsible for the existence of this transition point. The lateral inertia confinement in a SHPB test may play an important role for this transition phenomenon, as discussed in

Fig. 2. Strain-rate influence on DIF measured by SHPB.

Section 2.3. A qualitative study based on Grote et al. (2001)'s test results will be presented in Section 3 using FEM to give further supporting evidence for the important role of lateral confinement in a SHPB test.

2.3. Lateral confinement in a SHPB test

The physical mechanisms about the strain-rate effect on DIF of concrete have not been fully understood. At least, two factors, i.e., the viscoelastic character of the hardened cement paste and the time-dependent micro-crack growth, may contribute to the macroscopic DIF sensitivity to strain-rate. It also shows that the presence of the free water in the material may lead to a strain-rate effect similar to the Stefan effect (Rossi et al., 1994). It seems that concrete samples are not strain-rate sensitive below strain-rate of 10^0 s^{-1} unless free water is present. However, these mechanisms are not able to explain the observed rate dependence of DIF of concrete at high strain-rates ($>10^1$–10^2 s^{-1}) on dry samples.

A very important factor, which may cause the dynamic strength enhancement of concrete with increase of strain-rate, is the lateral confinement in a SHPB test. The lateral confinement comes from both the contact surface restriction and the lateral inertia during the rapid compression. The influence of the lateral confinement on SHPB measurement is normally ignored for metallic specimens because the contact friction is ultimately reduced using lubricant and the lateral inertia induced lateral confinement does not influence the flow stress due to an important fact that the metal plasticity is hydrostatic-stress-independent. However, the stress response of concrete-like material is hydrostatic-stress-dependent, and therefore, it has completely different response to the lateral confinement. The fact is that the compressive strength of a concrete-like material can be largely enhanced by the lateral confinement. Presently, a numerical simulation that considers strain-rate effect on the DIF of concrete in a material model has been regarded as an advanced simulation if the impact or explosive loading is involved in the simulated phenomenon. When the conventional SHPB technique, which has become an important means to obtain the dependence of DIF of concrete on strain-rate in the range of 10^1–10^3 s^{-1}, is used to test a concrete-like material, the lateral confinement due to lateral inertia will greatly enhance the measured uniaxial compressive stress. Unfortunately, such strength enhancement due to the lateral confinement in SHPB test is frequently interpreted as the strain-rate enhancement in most of experimental publications, e.g., Grote et al. (2001), and has been subsequently implemented into the concrete model for a numerical simulation.

There are few publications to note this issue and to study the development of the lateral confinement in a SHPB test for concrete specimen. In their literature review about the compressive behaviour of concrete at high strain-rates, Bischoff and Perry (1991) summarized the scatter evidences about the lateral inertia confinement influence on the compressive strength of concrete-like materials in a dynamic test. This phenomenon was firstly noted by Brace and Jones (1971) when they tested the dynamic compressive strength of rocks. They suggested that the sharp increase in the compressive strength of brittle materials may not be 'real', but comes from a result of the transition from a uniaxial stress state to a uniaxial strain state (Brace and Jones, 1971; Bischoff and Perry, 1991). This viewpoint is supported by several studies on rock, e.g., Janach (1976), Glenn and Janach (1977) and Young and Powell (1979). However, opinions are still divided about whether the strain-rate effect on the stress increase in rock is 'real' or due to lateral inertia confinement (Bischoff and Perry, 1991).

Compression tests on concrete using SHPB showed that the lateral inertia confinement is negligible for strain-rates up to 10^2 s^{-1} (Malvern et al., 1985). Gupta and Seaman (1979) tested concrete specimens in plane strain state under both quasi-static loading condition and strain-rates around 10^4 s^{-1} using plate impact. They noted that the compressive strength increase at a strain-rate of 10^4 s^{-1} is much less the prediction from the CEB recommendations (Comite Euro-International du Beton, 1993). The formula recommended by CEB gives a sharp increase of DIF when the strain-rate is greater than 30 s^{-1}. This

recommendation was questioned by Bischoff and Perry (1991), i.e., such sharp increase of the concrete strength may be due to the change of the specimen response from the uniaxial stress state to the uniaxial strain state rather than a strain-rate effect.

Based on an assumption that the specimen deformation is uniform and therefore the radial and hoop strains are independent of the radial coordinate, a quadratic expression of the radial stress distribution was obtained by Tang et al. (1992) to estimate the lateral inertia confinement in a cylindrical concrete specimen in SHPB test. It was shown that the magnitude of the lateral inertia confinement is not larger than 0.1–0.2% of the magnitude of the compressive strength in their SHPB tests within a range of strain-rates up to 200 s^{-1}. It was concluded that the influence of the lateral inertia confinement on SHPB test results is trivial in these SHPB tests (Tang et al., 1992). However, this conclusion is questionable if the validity of the assumption in their analyses is not satisfied.

Georgin et al. (1998) simulated the force transmission through a cylindrical specimen when the velocities on the two faces of the cylinder are imposed. Both fixed and free end conditions were examined as two extreme situations. Two different material models were used, i.e., a Drucker–Prager model, which is hydrostatic-stress-dependent, and von Mises model, which is hydrostatic-stress-independent. The influences of the axial inertia force, lateral inertia confinement and boundary conditions on the force transmission through a concrete cylinder were briefly studied. It shows that confinement may be developed in a SHPB test, which could lead to an apparent strength increase when the specimen material is hydrostatic-stress-dependent. A similar problem was simulated by Donze et al. (1999) using a 3D discrete-element method where the input data are the velocities at both ends of the cylindrical specimen and the output data are the computed forces on these two end faces. It shows that the transmitted force through the concrete cylinder could be increased, thus, leading to an apparent strain-rate effect that is actually due to the lateral inertial confinement.

These limited studies support Bischoff and Perry (1991)'s claim that the strength enhancement may be caused partly by a transition from a state of uniaxial stress to uniaxial strain. When the stress state in the cylindrical specimen in a SHPB test is deviated from the uniaxial stress state, the apparent compressive strength will definitely increase if the tested material is hydrostatic-stress-dependent. Further studies are necessary to confirm this new explanation for the strain-rate sensitivity of concrete and concrete-like materials at high strain-rates and to locate the transition point of the apparent strain-rate sensitivity for each type of concrete-like materials.

3. Numerical SHPB experiment based on FEA

3.1. Methodology

Two important issues should be addressed in the numerical verification of a SHPB test. First of all, it is necessary to prove that the obtained SHPB test results represent the material property of the tested specimen rather than the structural response of the specimen in a SHPB system. Secondly, the apparent strain-rate effect on the stress measured in a SHPB test should be due to material strain-rate sensitivity rather than other causes.

A "reconstitution method" will be used in the present study. This methodology requires a given constitutive model for the tested material of the specimen. Normally, the dynamic constitutive equation of the tested material is unavailable before conducting dynamic material test. The flow stress dependence on the strain-rate is secondary to the flow stress dependence on strain within a range of strain-rate and the strain-rate-dependence is usually considered through an enhancement factor $R(\dot{\varepsilon})$

$$\sigma_d = \sigma_s(\varepsilon)R(\dot{\varepsilon}) \tag{6}$$

e.g., Cowper–Symonds relation (Jones, 1997) and Jonhson–Cook model (Johnson and Cook, 1983). Therefore, a stress–strain relation in quasi-static uniaxial compression and its corresponding quasi-static constitutive equation could be used in the numerical verification. The numerically tested material can be considered as strain-rate-independent. The specimen and SHPB pressure bars are simulated as a structural problem to get the so-called ''reconstituted'' stresses and strains based on SHPB formulas, which can be used to obtain a ''reconstituted'' axial stress–strain relation. The deviation between this ''reconstituted'' axial stress–strain relation and the input axial stress–strain relation indicates the error due to the violation of the fundamental assumptions in a SHPB test. This methodology has been adopted by Bertholf and Karnes (1975) and by Meng and Li (2002) to estimate the accuracy of the SHPB test for metallic specimens. The advantage of using a strain-rate-independent stress–strain relation as the input is that all discrepancies between the reconstituted stress–strain curve and the input stress–strain curve are not due to the strain-rate effect, but due to other negative factors in a SHPB test, which should be correctly interpreted in the analyses of the SHPB test results. Meanwhile, the quasi-static stress–strain relation is able to capture the main feature of the stress–strain relation of the tested material since the strain-rate effect is normally secondary.

3.2. Constitutive equation of concrete

A typical uniaxial stress–strain relation of concrete or concrete like material is shown in Fig. 3. A linear stress–strain relation exists between the ultimate tensile strength (f_{ts}) and the elastic limit (σ_c). The stress–strain relation becomes non-linear due to the existence of micro-cracks between the elastic limit and the ultimate compression strength (f_{cs}), which is followed by a strain softening phase and a residual strength phase. The identification of a constitutive model of concrete or concrete-like material requires test results from a uniaxial stress–strain relation and its dependence on the stress triaxility.

Various material models have been proposed to include the above mentioned features of concrete or concrete-like materials with various simplicities and application purposes, e.g., the plasticity concrete model in LS-DYNA (Malvar et al., 1997) and ABAQUS (Park et al., 2001) and the hypoelastic model in ADINA (Tedesco et al., 1997). As advanced constitutive models introduce more experimental parameters and increase computational difficulties, a simplified model may give more accurate and efficient predictions if it is representative to the characteristics of the studied problem.

Drucker–Prager model (Drucker and Prager, 1952) has been extended to model the behavior of concrete or concrete-like materials, which is capable of providing phenomenological account for the pressure-dependent flow due to the internal friction, a typical feature of concrete or concrete-like materials. It allows

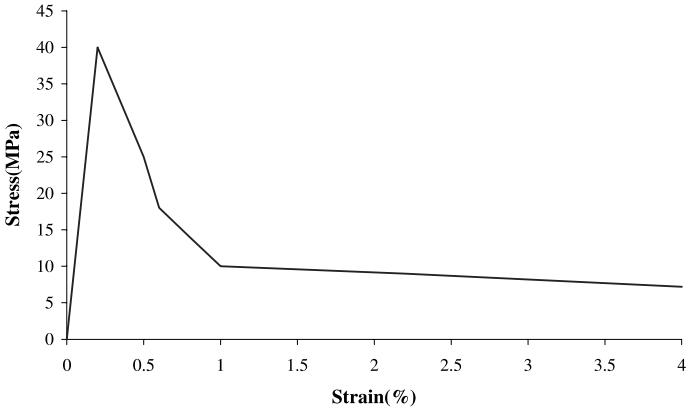

Fig. 3. Quasi-static uniaxial stress–strain curve of mortar.

the evolution of the deformation to be tracked through both the strain hardening and the strain softening within the framework of finite deformation kinematics. Both the Drucker–Prager model and the FE modeling used in the present study are well established. This ensures that the new discovery on the strain rate dependence of DIF is not influenced by the uncertainties of the numerical SHPB experiment, but comes from other sources, which will be identified and studied in the present paper.

The linear Drucker–Prager model in ABAQUS (ABAQUS theory manual version 5.8) was used by Park et al. (2001) to simulate plate impact tests on concrete and mortar. Strain-rate sensitivity was introduced by scaling the quasi-static flow stress through DIF obtained from standard SHPB test (Grote et al., 2001). However, according to the discussion in Section 2.3, SHPB results for concrete or concrete-like materials may be misinterpreted due to the existence of lateral inertia confinement and their authenticity is questionable, which will be shown in the following simulation on the response of mortar specimen in SHPB tests using the same linear Drucker–Prager model and the FEM code ABAQUS/Explicit as those used by Park et al. (2001).

The yielding criterion in a linear Drucker–Prager model, as shown in Fig. 4, is

$$F = t - p\tan\beta - d = 0 \tag{7}$$

where β is the slope of the linear yield surface in the p–t stress plane and β is commonly referred to as the friction angle of the material, $d = \left(1 - \frac{1}{3}\tan\beta\right)\sigma_c$ if the hardening is defined by the uniaxial compression yield stress σ_c. $p = -\frac{1}{3}\mathrm{trace}(\sigma)$ is the equivalent hydrostatic stress and t is a deviatoric stress measure defined by

$$t = \frac{q}{2}\left[1 + \frac{1}{K} - \left(1 - \frac{1}{K}\right)\left(\frac{r}{q}\right)^3\right] \tag{8}$$

where $q = \sqrt{\frac{3}{2}(S:S)}$ is the von-Mises equivalent stress, $r = \left(\frac{9}{2}S:S:S\right)^{\frac{1}{3}}$ and $S = \sigma + pI$ is the deviatoric stress.

The flow rule of the linear Drucker–Prager model is

$$\mathrm{d}\varepsilon^p_{ij} = \frac{\mathrm{d}\bar{\varepsilon}^p}{c}\frac{\partial G}{\partial \sigma_{ij}} \tag{9}$$

where $\bar{\varepsilon}^p$ is the equivalent plastic strain, $c = 1 - (1/3)\tan\psi$ and the flow potential is

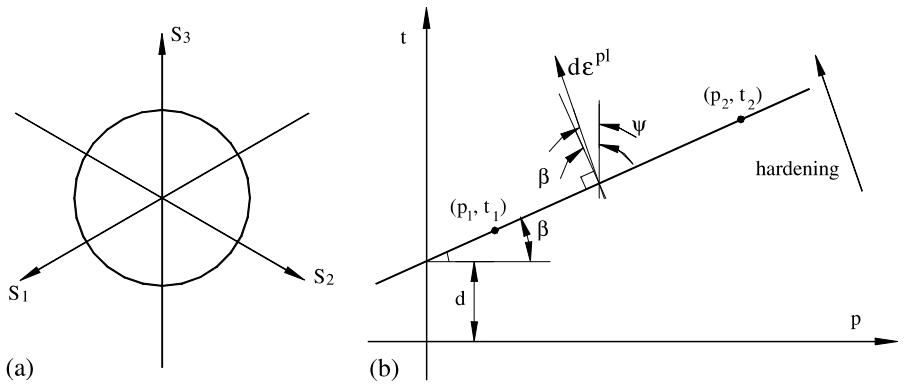

Fig. 4. Drucker–Prager failure criterion: (a) typical failure surface in the deviatoric plane and (b) failure surface and flow direction in the p–t plane.

$$G = t - p\tan\psi \tag{10}$$

in which, ψ is the dilation angle in the p–t plane. The geometrical interpretation of ψ is shown in Fig. 4(b).

3.3. Numerical model

A description of the examined problem is illustrated in Fig. 5. The dimensions of the set-up are the same as those used by Grote et al. (2001) for comparison purpose.

The calculations are performed using the general-purpose finite element code ABAQUS/Explicit version 5.8 with element type CAX4R (axis symmetric element, reduced integration). The specimen is meshed into 30 elements along the radius and 30 elements in the axial direction. Each elastic pressure bar is represented by 10 elements along the radius and 800 elements in the axial direction with finer meshes near the bar/specimen interfaces, as shown in Fig. 6. Finer meshes were examined in several trial simulations, which did not bring significant difference comparing with the results based on the current mesh. The sliding is permitted between the specimen and the pressure bar and a constant friction coefficient is assumed. An automatic time-integration scheme offered by ABAQUS/Explicit is used throughout the simulation.

The material properties and the dimensions of SHPB apparatus employed in the present study are listed in Table 1. The uniaxial quasi-static stress–strain curve of the specimen is shown in Fig. 3, which is simplified from Maher and Darwin (1980). As the main concern of the study is the ultimate uniaxial compressive strength of the concrete rather than the post-failure process, the stress–strain relation before the ultimate compressive strength of the mortar is simplified into a linear elastic relation with the ultimate compressive strength of 40 MPa and the ultimate strain of 0.2%, followed by a strain softening region. It is evident that the ultimate strength is regarded as the yield stress here.

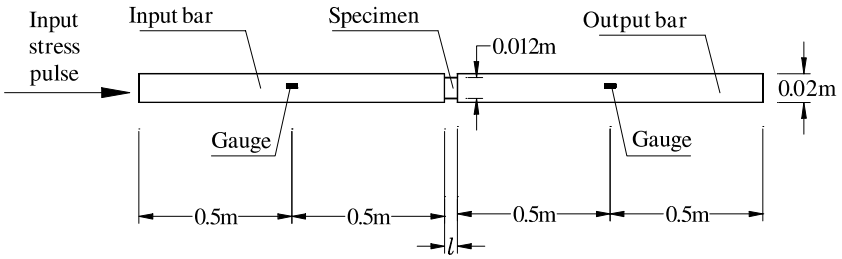

Fig. 5. Configuration of the SHPB set-up for numerical simulation.

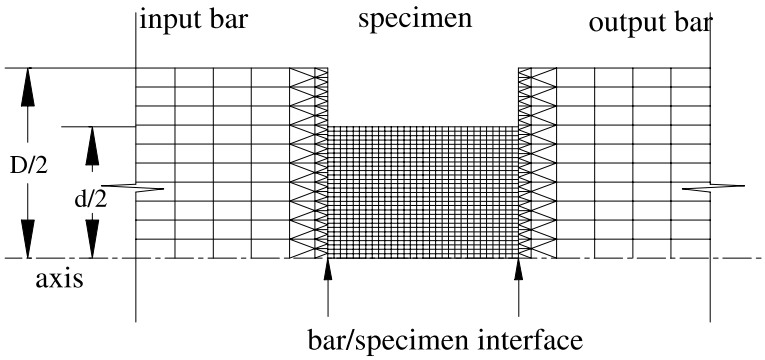

Fig. 6. Axisymmetric finite element model of the specimen and the pressure bars.

Table 1
Material properties and the dimensions of SHPB

	Dimensions		Material properties			
	Length (m)	Diameter (m)	Material	E (MPa)	ρ (kg/m^3)	v
Pressure bar	1.0	0.02	Steel	2×10^5	7800	0.3
Specimen	Varies	0.012	Mortar	2×10^3	2000	0.2

Triaxial testing data are necessary to determine material parameters for concrete and concrete-like materials. A method to determine these parameters from triaxial test data has been provided by Drucker–Prager model in ABAQUS/Explicit. A triaxial compressive test is normally conducted by compressing a specimen that is confined by a constant pressure. Thus, the principal stresses are all negative with $0 \geqslant \sigma_1 = \sigma_2$ and $0 \geqslant \sigma_3$, so that

$$p = -\frac{1}{3}(2\sigma_1 + \sigma_3) \tag{11}$$

and

$$t = \sigma_1 - \sigma_3 \tag{12}$$

when $K = 1$ (Note: specimen response is insensitive to K according to Park et al. (2001)), and

$$\beta = \arctan\left(\frac{t_1 - t_2}{p_1 - p_2}\right)$$

where t_1, t_2 and p_1, p_2 are the coordinate values at point 1 and 2 in p–t plane shown in Fig. 4(b). Based on the data of actual triaxial compression tests (US Dept. of the Interior Bureau of Reclamation, 1954; Dahl, 1992; Zhang, 2001), the real value of β for mortar ranges from 40–60°, and therefore, $\beta = 50°$ is used in the numerical simulation in the current study. In their simulation of plate impact of mortar, Park et al. (2001) found that ψ has limited influence on the specimen response. In the present research, the influence of ψ on DIF in a SHPB test is almost negligible according to parametric studies. Thus, an associated flow law, i.e., $\psi = \beta$, is used in the following simulations.

4. Numerical results and discussion

Instead of modeling the collision between an impact bar and the incident pressure bar, a stress pulse of trapezium shape is inputted into the incident pressure bar. The rising time of the pulse varies from 0 to 180 μs, the pulse duration varies from 30 to 240 μs and the stress intensity varies from 45 to 1000 MPa. Different combinations of the pulse parameters are used to obtain desired strain rates at the measured ultimate stress of the SHPB test. The actual shape of the input pulse will be changed when it reaches the specimen due to the wave dispersion. Nevertheless, trial simulations have shown that the ultimate strength measured from a numerical SHPB test depends mainly on the measured strain rate at the ultimate stress. The influence of the pulse shape on the measured ultimate strength is not explicit, but through the measured strain rate at the ultimate stress. However, both the rising time and the stress intensity of the input pulse could be adjusted to change the strain rate in a SHPB test.

Fig. 7 gives the numerical strain histories obtained at strain gauge locations in the SHPB set-up in Fig. 5 with the specimen length of $l = 60$ mm, the length–diameter ratio of $l/d = 0.5$, the friction coefficient of zero and the nominal strain-rate of 390 s^{-1}. The initial compressive wave ε_I is partly reflected back into the

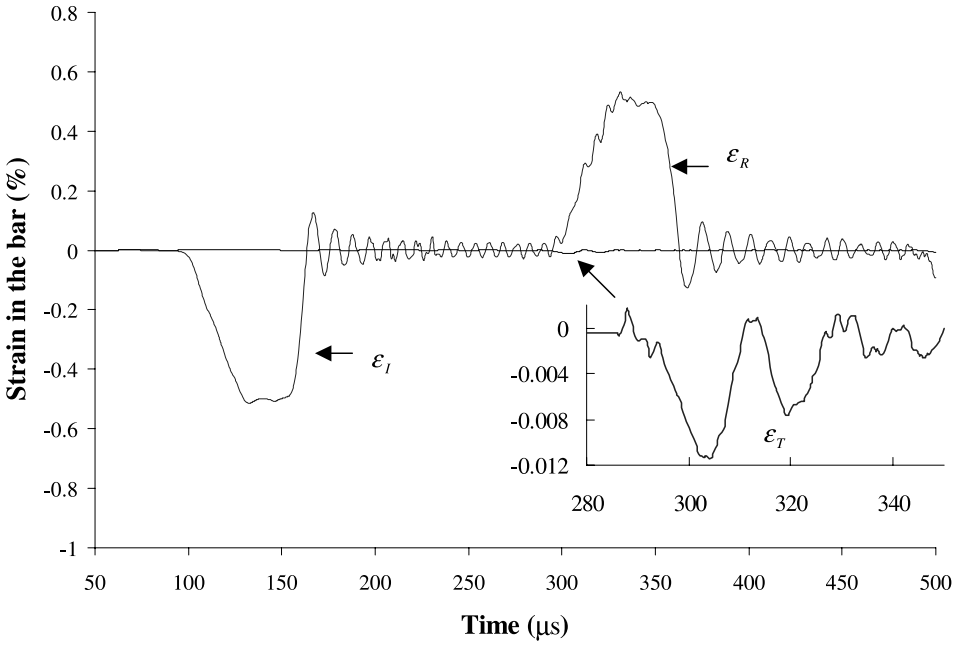

Fig. 7. Strain histories measured by gauges in a numerical SHPB test.

incident bar as a tensile wave ε_R and partly transmitted into the transmitter bar through the specimen as a compressive wave ε_T.

The stress–strain curves obtained from the strain histories through Eqs. (1a–c) and the hydrostatic stress at the same time at two different nominal strain-rates of 27 and 390 s^{-1} are shown in Figs. 8 and 9, respectively. It shows that the stress–strain curve at the nominal strain-rate of 27 s^{-1} in Fig. 8 fits the input uniaxial stress strain curve very well, especially before the ultimate compressive strength is reached. No apparent strain-rate effect is observed and the hydrostatic stress keeps about 1/3 of the uniaxial compressive stress. It transpires that other two principal stresses σ_1 and σ_2 are both zero at the nominal strain-rate of 27 s^{-1} and the stress state in majority of the specimen material is uniaxial in this numerical SHPB test. In all

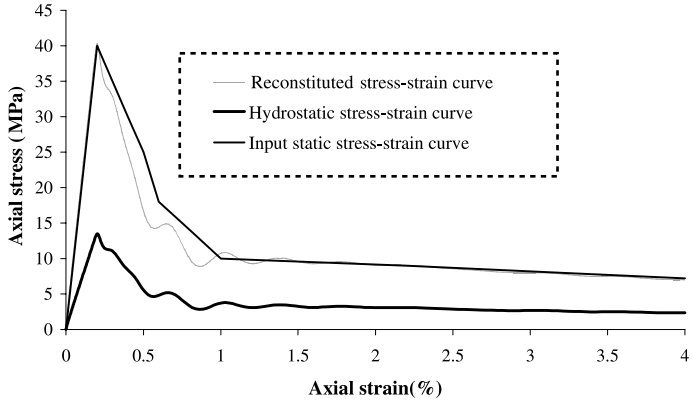

Fig. 8. The axial stress versus the axial strain and the hydrostatic stress versus the axial strain at a nominal strain-rate of 27 s^{-1}.

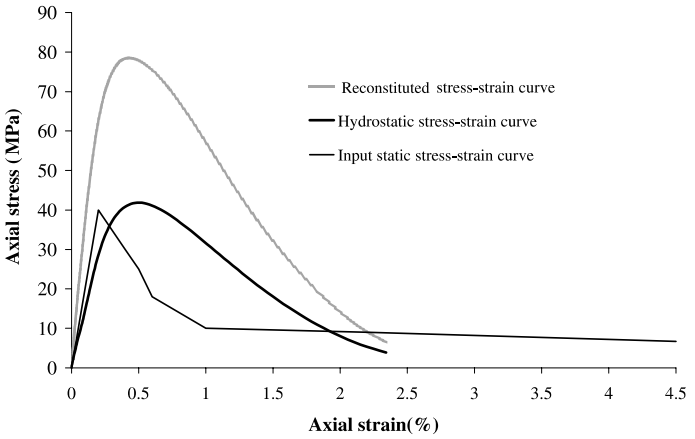

Fig. 9. The axial stress versus the axial strain and the hydrostatic stress versus the axial strain at a nominal strain-rate of 390 s^{-1}.

numerical simulations of SHPB tests associated with a low strain-rate, the hydrostatic stress of the tested specimens is uniform and the lateral confinement due to the lateral inertia is insignificant. No apparent strain-rate effects for the current material model were observed in the numerical SHPB tests at lower strain-rates.

However, with the increase of the nominal strain-rate, the lateral confinement due to the lateral inertia becomes significant, Fig. 9 shows the SHPB outputs of the stress–strain relation and the corresponding average hydrostatic stress in the specimen at nominal strain-rate of 390 s^{-1}. Both the ultimate strength and the Young's modulus increase dramatically. The measured ultimate compressive strength is almost twice of the corresponding quasi-static value. So does the Young's modulus. In a real SHPB test, these results are attributed to the strain-rate effect. As the constitutive relation in the numerical simulations of a SHPB test is strain-rate-independence, the observed apparent strain-rate effects are not genuine, but due to other reasons.

When we examine the average hydrostatic stress in the specimen, its value is more than half of the compressive stress, which means that other two principal stresses are not zero, i.e., $\sigma_1 = \sigma_2 \neq 0$. Lateral inertia becomes significant in the specimen, which restricts the radial expansion of the specimen and causes lateral confinement. According to Drucker–Prager model, the uniaxial compressive strength increases with hydrostatic stress. Fig. 10 shows the hydrostatic stress contour within the tested specimen at a nominal strain of $\varepsilon = 0.081\%$. It is obvious that the center of the specimen, which is restricted by the surround material, has much higher hydrostatic stress. The fact that the apparent ultimate compressive strength and the apparent Young's modulus increase with strain-rate is actually a pseudo-strain-rate effect, which is caused by the lateral inertia in the specimen of a SHPB test for hydrostatic-stress-dependent materials.

As the commonly accepted slenderness ratio (l/d) of the specimen in SHPB tests for concrete and concrete-like materials is from 0.3 to 1.0. The pseudo-strain-rate effects on DIF of mortar are simulated and presented in Fig. 11 for three different slenderness ratios. SHPB test results from independent publications are also presented for comparison purpose. It is interesting to find that DIF obtained from SHPB tests follows the predicted DIF from numerical SHPB simulations.

Based on Fig. 11, the apparent ultimate compressive strength begins to increase at the average nominal strain-rate of 10 s^{-1} and a significant increase is observed when strain-rate is beyond a transition point around 10^2 s^{-1}. However, the differences between the results for different slenderness ratios of

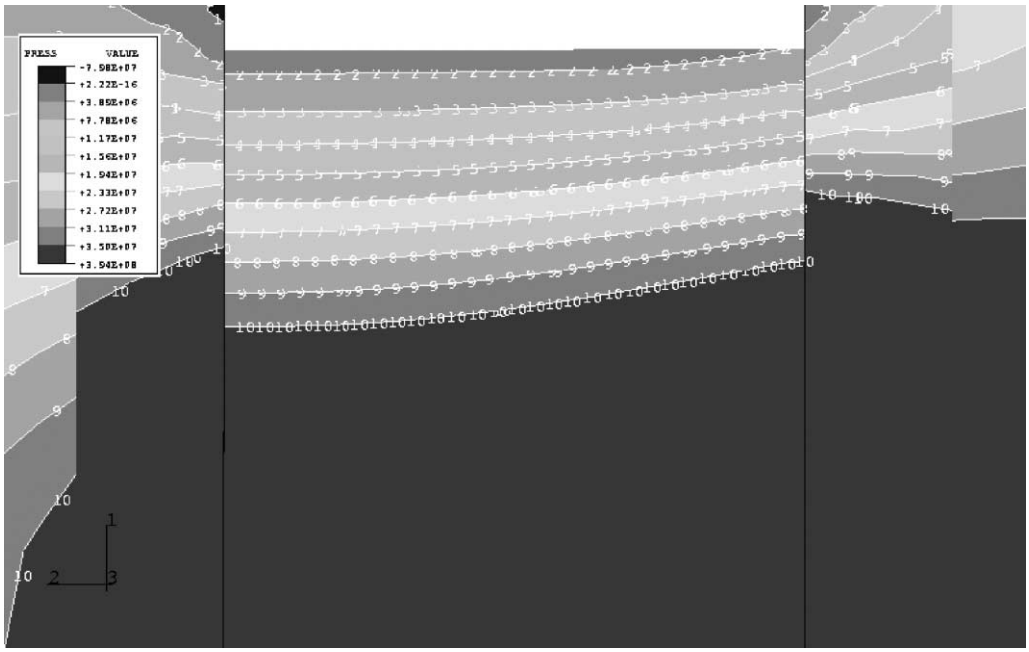

Fig. 10. The contour of the hydrostatic stress in the specimen corresponding to a nominal strain of $\varepsilon = 0.081\%$ at a nominal strain-rate of 390 s^{-1}.

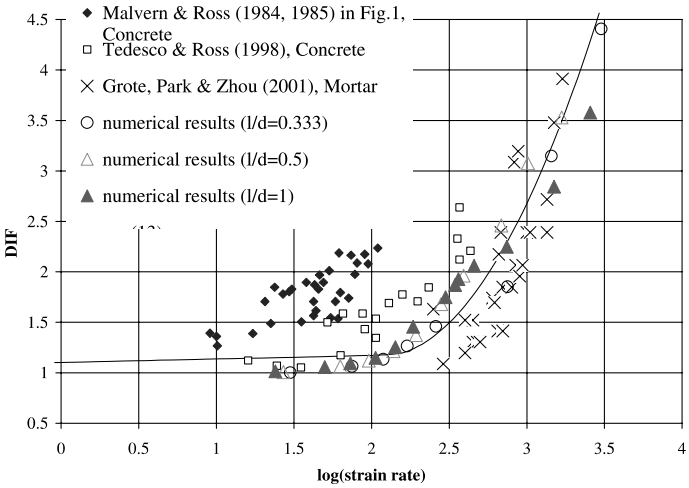

Fig. 11. Comparison between the predicted DIF and the measured DIF from SHPB tests.

the specimen are not significant within the examined values of l/d and the strain-rates in the present study.

Define the strain-rate of 10^{-4} s^{-1} as the quasi-static strain-rate, all the numerical results for three different slenderness ratios can be described by the following linear and quadratic polynomial relationships of the logarithm strain-rate,

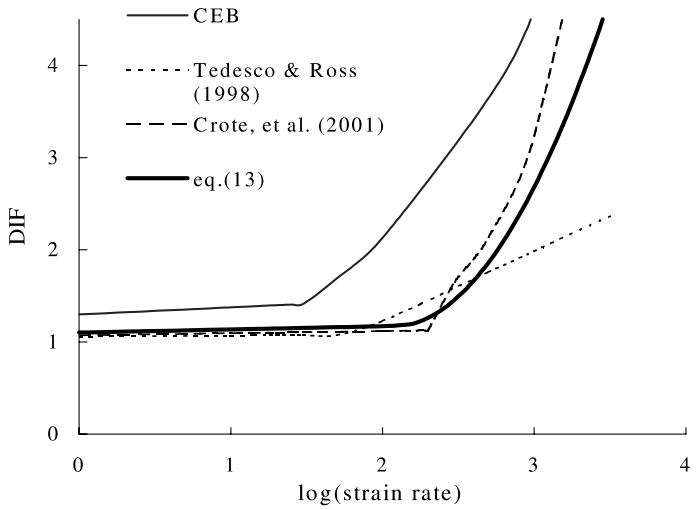

Fig. 12. Comparison between other DIF recommendations and the predicted DIF formulation.

$$R = \begin{cases} 1 + (\log \dot{\varepsilon} + 3) \times 0.03438 & \text{for } \dot{\varepsilon} \leqslant 10^2 \text{ s}^{-1} \\ \beta_0 + \beta_1 \log(\dot{\varepsilon}) + \beta_2 \log^2(\dot{\varepsilon}) & \text{for } \dot{\varepsilon} > 10^2 \text{ s}^{-1} \end{cases} \tag{13}$$

in which, $R = \text{DIF} = f_{cd}/f_{cs}$ is the ratio of the apparent dynamic strength f_{cd} to the quasi-static strength f_{cs}. $\beta_0 = 8.5303$, $\beta_1 = -7.1372$ and $\beta_2 = 1.729$ are determined by least-squares method according to data in Fig. 11.

Eq. (13) is compared with the CED recommendation, Eqs. (3a) and (3b), Tedesco and Ross (1998)'s recommendation, Eqs. (4a) and (4b), and Grote et al. (2001)'s recommendation, Eqs. (5a) and (5b), as shown in Fig. 12. It shows that the DIF based on the CEB recommendation is much larger than other two recommendations from Tedesco and Ross (1998) and Grote et al. (2001) in the strain-rate range of 10^1–10^2 s^{-1}. Eq. (13) gives a good average of Tedesco and Ross (1998)'s recommendation and Grote et al. (2001)'s recommendation at strain-rates between 10^1 and 10^3 s^{-1}. However, Eq. (13) represents the pseudo-strain-rate-dependence, which should be eliminated from the measured DIF in actual SHPB tests. Generally, a relation between DIF and the strain-rate is insensitive to f_{cs} since DIF is a dimensionless parameter and therefore results obtained for $f_{cs} = 40$ MPa may be applicable to other compressive strengths of similar concrete or concrete-like materials. However, a confident conclusion on this issue requires further studies.

It is well known that the SHPB results are particularly susceptible to the friction between the bar/specimen interfaces. Bertholf and Karnes (1975) performed a comprehensive two-dimensional numerical analysis about SHPB test and described the friction effect quantitatively. They concluded that the friction effect could be effectively minimized if the ends of the specimen are well lubricated. This conclusion is made for the metal specimen whose friction coefficient is normally smaller than the friction coefficient of a concrete or concrete-like material. For concrete or concrete-like specimens, the surface of the specimen is much coarser than the surface of a metallic specimen, and thus, the friction effect cannot be totally neglected even though the interface is lubricated.

In order to investigate the friction effect on the measurement of DIF of concrete or concrete-like materials through SHPB, a series of parametric analyses using the present FEM model were made for the mortar specimen. A slenderness ratio of $l/d = 0.5$ is used in all simulations. Friction coefficients vary from 0.0 to 0.7. It is shown in Fig. 13 that the apparent uniaxial compressive strength of the mortar is enhanced by friction effect that supplies another restraint to the lateral motion of the specimen material. However, the

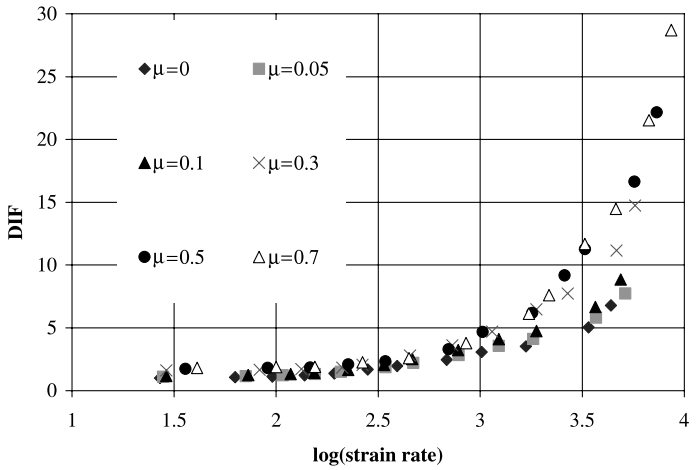

Fig. 13. Contribution of the friction to the dependence of DIF on strain-rate in numerical SHPB tests.

influence of the friction coefficient on DIF is insignificant when μ is less than 0.1. Practically, the friction coefficient between the specimen and the pressure bars can be reduced to this value by applying lubrication properly. Fig. 13 indicates that, when friction coefficient is larger than 0.2, it may enhance DIF considerably in a SHPB test, which may also be misinterpreted as strain-rate effect. Thus, the validity of a SHPB test should be justified before it is implemented into material models. The present study results shows that DIF of concrete or concrete-like materials measured from SHPB at nominal strain-rates beyond 10^2 s^{-1} is influenced strongly by the existence of the lateral confinement due to the lateral inertia, which does not represent the real strain-rate-dependence of the tested material. Thus, great pre-caution should be paid when using a strain-rate-dependence model of concrete or concrete-like materials in both structural design and simulation.

5. Conclusions

Numerical simulations show that the lateral inertia force of the specimen increases the lateral confinement in a SHPB test, which causes an apparent increase of the DIF for concrete and concrete-like materials whose stress–strain relation can be represented by a hydrostatic-stress-dependent constitutive law, e.g., Drucker–Prager model. This effect becomes significant when the nominal strain-rate is around 10^2 s^{-1}, which coincides with the experimentally obtained transition point from a weak strain-rate-dependency to a strong strain-rate-dependency. Thus, the observed strain-rate sensitivity from 10^2 s^{-1} in SHPB test is a pseudo-strain-rate effect, which is caused actually by the material strength sensitivity to the hydrostatic-stress due to the lateral inertia confinement. Many applications misinterpreted this pseudo-strain-rate effect as real strain-rate effect in the design and numerical models, which may overestimate the dynamic compressive strength of concrete or concrete-like materials.

Further studies are necessary for a fully understanding about the strain-rate effect on the ultimate uniaxial compressive strength of concrete and concrete-like materials in SHPB tests. Both experiments and numerical studies may offer more information to separate pseudo-strain-rate effects from genuine strain-rate effects in dynamic material property tests, which is important for material model identifications.

References

Abrams, D.A., 1917. Effect of rate of application of load on the compressive strength of concrete. ASTM J. 17, 364–377.

Bell, J.F., 1966. An experimental diffraction grating study of the quasi-static hypothesis of the SHPB experiment. J. Mech. Phys. Solids 14, 309–327.

Bertholf, L.D., Karnes, C.H., 1975. Two dimensional analysis of the split Hopkinson pressure bar system. J. Mech. Phys. Solids 23, 1–19.

Bischoff, P.H., Perry, S.H., 1991. Compression behavior of concrete at high strain-rates. Mater. Struct. 24, 425–450.

Brace, W.F., Jones, A.H., 1971. Comparison of uniaxial deformation in shock and static loading of three rocks. J. Geomech. Abstr. 13 (6), 4913–4921.

Comite Euro-International du Beton, 1993. CEB-FIP model code 1990, Redwood Books, Trowbridge, Wiltshire, UK.

Dahl, K.K.B., 1992. A failure criterion for normal and high strength concrete, no. R-286. Department of Structural Engineering, Technical University of Denmark.

Davies, E.D.H., Hunter, S.C., 1963. The dynamic compression testing of solids by the method of the split Hopkinson bar. J. Mech. Phys. Solids 11, 155–179.

Donze, F.V., Magnier, S.A., Daudeville, L., Mariotti, C., Davenne, L., 1999. Numerical study of compressive behaviour of concrete at high strain-rates. ASCE J. Engng. Mech. 125, 1154–1163.

Drucker, D.C., Prager, W., 1952. Soil mechanics and plastic analysis or limit design. Quart. Appl. Math. 10, 157–165.

Fu, H.C., Erki, M.A., Seckin, M., 1991a. Review of effects of loading rate on concrete in compression. ASCE J. Struct. Engng. 117 (12), 3645–3659.

Fu, H.C., Erki, M.A., Seckin, M., 1991b. Review of effects of loading rate on reinforced concrete. ASCE J. Struct. Engng. 117 (12), 3660–3679.

Goldsmith, W., Polivka, M., Yang, T., 1966. Dynamic behaviour of concrete. Exp. Mech. 6, 65–79.

Georgin, J.F., Reynouard, J.M., Merabet, O., 1998. Modeling of concrete at high strain rate, In: de Borst, Bicanic, Mang, Meschhke (Eds.), Computational Modeling of Concrete Structures, Rotterdam, pp. 593–601.

Glenn, L.A., Janach, W., 1977. Failure of grnite cylinders under impact loading. Int. J. Fract. 13, 301–317.

Grote, D.L., Park, S.W., Zhou, M., 2001. Dynamic behavior of concrete at high strain-rates and pressures: I. Experimental characterization. Int. J. Impact Engng. 25, 869–886.

Gupta, Y.M., Seaman, L., 1979. Local response of reinforced concrete to missile impact, Final Report, EPRI NP-1217, Project 393-1, Palo Alto.

Janach, W., 1976. The role of bulking in brittle failure of rocks under rapid compression. Int. J. Rock Mech. Mining Sci. Geomech. Abstr. 13 (6), 177–186.

Johnson, G.R., Cook, W.H., 1983. A constitutive model and data for metals subjected to large strains, high strain rates and high temperatures, Proc. 7th Int. Symp. Ballistics, Am. Def. Prep. Org. (ADPA), The Hague, Netherlands, pp. 541–547.

Jones, N., 1997. Structural impact. Cambridge University Press, Cambridge, Paperback edition.

Maher, A., Darwin, D., 1980. Mortar constitutive of Concrete Under Cyclic Compression, A Report on Research Sponsored by The National Science Foundation Research Grants, ENG 76-09444, CME 79-18414, University of Kansas Lawrence, Kansas, October 1980.

Malvern, L.E., Ross, C.A., 1985. Dynamic response of concrete and concrete structures, Second Annual Technical Report, AFOSR contract no. F49620-83-K007.

Malvern, L.E., Jenkins, D.A., Tianxi, T., Ross, C.A., 1985. Dynamic compressive testing of concrete. In: Proceeding of the Second Symposium on the Interaction of Non-nuclear Munitions with Structures, Panama City Beach, FL. pp. 397–402.

Malvar, L.J., Crawford, J.E., Wesevich, J.W., Simons, D., 1997. A plasticity concrete material model for DYNA3D. Int. J. Impact Engng. 19 (9–10), 847–873.

Meng, H., Li, Q.M., 2002. Correlation between the accuracy of a SHPB test and stress uniformity based on numerical experiments. International Journal of Impact Engineering, in press.

Park, S.W., Xia, Q., Zhou, M., 2001. Dynamic behavior of concrete at high strain rates and pressures: II. Numerical simulation. Int. J. Impact Engng. 25, 887–910.

Ross, C.A., Thompson, P.Y., Tedesco, J.W., 1989. Split-Hopkinson pressure-bar tests on concrete and mortar in tension and compression. ACI Mater. J. 86, 475–481.

Ross, A., Tedesco, J.W., Kuennen, S.T., 1995. Effects of strain rate on concrete strength. ACI Mater. J. 92 (1), 37–47.

Ross, A., Jerome, D.M., Tedesco, J.W., Hughes, M.L., 1996. Moisture and strain rate effects on concrete strength. ACI Mater. J. 93 (3), 293–300.

Rossi, P., Van Mier, J.G.M., Toutlemonde, F., Le Maou, F., Boulay, C., 1994. Effect of loading rate on the strength of concrete of concrete subjected to uniaxial tension. Mater. Struct. 27, 260–264.

Tang, T., Malvern, L.E., Jenkins, D.A., 1992. Rate effects in uni-axial dynamic compression of concrete. ASCE J. Engng. Mech. 118 (1), 108–124.

Tedesco, J.W., Powell, J.C., Ross, C.A., Hughes, M.L., 1997. A strain-rate-dependent concrete material model for ADINA. Comput. Struct. 64 (5/6), 1053–1067.

Tedesco, J.W., Ross, C.A., 1998. Strain-rate-dependent constitutive equations for concrete. ASME J. Press. Vessel Technol. 120, 398–405.

US Dept. of the Interior Bureau of Reclamation,1954. Triaxial Strength Tests of Neat Cement and Mortar Cylinders, Concrete Laboratory Report, no. C-779, Engineering Laboratories, Denver, November 1954.

Williams, M.S., 1994. Modeling of local impact effects on plain and reinforced concrete. ACI Struct. J. 91 (2), 178–187.

Young, C., Powell, C.N., 1979. Lateral inertia effects on rock failure in split Hopkinson-bar experiments, 20th US Symp. on Rock Mech., Univ. of Texas, Austin, Texas.

Zhang, J.G., 2001. Triaxial Behaviour of Cement Mortar Under Monotonic Loading, Master Thesis, School of Civil and Environmental Engineering, Nanyang Technological University.

Zhao, H., 1998. A study on testing techniques for concrete-like materials under compressive impact loading. Cement Concrete Compos. 20, 293–299.